

1 drmr: A Bayesian approach to Dynamic Range Models
2 in R

3 Lucas da Cunha Godoy¹² Alexa Fredston³ R. M. W. J. Bandara⁴
4 Mark Morales¹ Malin L. Pinsky¹

5 April 13, 2026

¹Department of Ecology and Evolutionary Biology, University of California Santa Cruz

²email: lucas@example.com

³Department of Ocean Sciences, University of California Santa Cruz

⁴Department of Ecology and Evolution, Rutgers University

Abstract

7 Predicting how species distributions will respond to environmental change is a critical chal-
8 lenge. Dynamic Range Models (DRMs) offer a powerful mechanistic approach by explicitly
9 modeling the influence of environmental drivers on demographic processes. However, the
10 widespread adoption of DRMs has been hindered by their inherent complexity and a critical
11 gap in the available software. While many tools can simulate range dynamics, none pro-
12 vide a user-friendly framework to statistically estimate the functional relationships between
13 environmental conditions and demographic rates from spatio-temporal data. To make this
14 approach more accessible, we introduce `drmr`, an open-source R package for building, fitting,
15 evaluating, and forecasting age-structured DRMs within a user-friendly Bayesian framework.
16 From spatio-temporal species observations, the `drmr` package allows users to explicitly es-
17 timate how environmental drivers affect demographic processes such as recruitment and
18 survival. We demonstrate the package's utility through case studies on summer flounder
19 (*Paralichthys dentatus*) and red-bellied woodpecker (*Melanerpes carolinus*). In both cases,
20 we fit DRMs with environment-dependent recruitment and survival. Additionally, we show
21 how the package visualizes estimated relationships between environmental conditions and de-
22 mographic rates. The `drmr` package bridges a critical gap between complex, process-explicit
23 models that are parameterized *a priori*, and statistically accessible correlative models that
24 are easily fit to data. By lowering the barrier to entry, it provides a powerful and accessi-
25 ble tool for ecologists to test mechanistic hypotheses and generate more robust ecological
26 forecasts in the face of global change.

27 *Keywords:* Climate change, Spatial prediction, Spatio-temporal modeling, Species distribu-
28 tion

1 Introduction

Predicting how species will respond to accelerating global environmental change remains one of the most critical challenges facing ecologists today (Urban et al., 2016). Knowledge of species' population dynamics is essential, as the demographic processes of reproduction, growth, mortality, and movement fundamentally govern species' distributions (Pagel and Schurr, 2012). Dynamic Range Models (DRMs) have emerged as promising tools for this purpose, explicitly linking demographic rates to environmental drivers within a hierarchical Bayesian framework (Pagel and Schurr, 2012). This approach allows for more robust predictions under novel environmental scenarios where traditional, correlative Species Distribution Models (SDMs) often fail (Fredston et al., 2025). Despite their conceptual appeal, the widespread application of DRMs has been limited by their inherent complexity and the computational challenges of fitting them to data (Evans and Moustakas, 2016; Uribe-Rivera et al., 2023).

The importance of biological mechanism in species distribution modeling inspired the development of several R packages. However, existing tools are designed for simulating species dynamics under pre-defined assumptions rather than statistically estimating the key relationships from data. For instance, `rangr` (Markowska et al., 2025), and `metaRange` (Fallert et al., 2025) are powerful virtual species platforms (VSP) but do not fit models to observational data. A few packages, such as `demoniche` (Nenzén et al., 2012), `MigClim` (Engler and Guisan, 2009), and `RangeShiftR` (Malchow et al., 2021; Bocedi et al., 2021) take the output of correlative SDMs to inform deterministic population dynamics or movement/dispersal algorithms. The `poems` package can fit spatially explicit metapopulation models to data through approximate Bayesian computation (ABC) (Fordham et al., 2021; Malchow et al., 2024). However, `poems` is exceptionally flexible and requires a steep learning curve for many users. It also relies on ABC, which is computationally expensive and more sensitive to simulation settings and prior constraints than the Markov Chain Monte Carlo (MCMC)-based inference used in `drmr`. To our knowledge, no existing package provides a flexible framework

Table 1: Comparison of R packages for spatial species dynamics and climate impacts. “SDM Packages” represents a wide range of standard options, such as `biomod`, `tinyVAST`, and `dismo`. The table evaluates these packages based on whether they explicitly represent demographic processes (Mechanistic), allow fitting spatially explicit models to data rather than just simulating them (Fits to spatial data), and can quantify uncertainty around parameter estimates and forecasts (Uncertainty). It also notes which packages accommodate environmentally-dependent demographic processes (Env-dem) and distinguishes those that use Markov Chain Monte Carlo rather than Approximate Bayesian Computation (ABC) for Bayesian inference (MCMC). Table symbols indicate if a feature is present (✓), absent (✗), or not applicable (·) to a given package.

Package	Mechanistic	Fits to spatial data	Uncertainty	Env-dem	MCMC
SDM Packages	✗	✓	✓	✗	✓
NicheMapR	✓	✗	✗	✗	·
RangeShiftR	✓	✓	✗	✗	·
rangr	✓	✗	✗	✗	·
steps	✓	✗	✗	✗	·
metaRange	✓	✗	✗	✗	·
SpatialDemography	✓	✗	✗	✗	·
MigClim	✓	✓	✗	✗	·
demoniche	✓	✓	✗	✗	·
poems	✓	✓	✓	✓	✗
drmr	✓	✓	✓	✓	✓

56 to directly estimate the functional relationships between environmental drivers and demo-
57 graphic rates within a single, integrated model. This step is essential for understanding why
58 ranges are shifting and for making credible forecasts. To illustrate the gap in functional-
59 ity across packages, from only simulation to environmentally-dependent population dynamic
60 models, we compare several packages in Table 1, including a broad category for the many
61 packages available for fitting more traditional SDMs (e.g., [Hijmans et al., 2024](#); [Thorson](#)
62 [et al., 2025](#)).

63 To bridge this application gap and make DRMs more accessible, we introduce `drmr`: an
64 open-source R ([R Core Team, 2024](#)) package for developing and applying DRMs using a
65 Bayesian framework. `drmr` is designed to substantially lower the barrier to applying this
66 class of models to real problems by providing a user-friendly interface for constructing,
67 fitting, and projecting age-structured DRMs. It leverages the power and efficiency of `Stan`

68 via the `cmdstanr` (Gabry et al., 2024) interface. The package offers flexibility, enabling
 69 users to easily relate environmental drivers to specific demographic rates like recruitment
 70 and survival. In this paper, we introduce the `drmr` framework and its capabilities. We do
 71 not attempt an exhaustive comparison against the myriad of modeling approaches already
 72 present in the literature.

73 2 Methods

74 We adopt the convention of representing random variables with capital letters and their
 75 observed values with lowercase letters. Formally, let $Y_{t,i}$ be a random variable representing
 76 the density of a focal species, with $y_{t,i}$ representing its realization, that is, what we actually
 77 observe. The sub-indices t and i stand for time and patch (or site), respectively. We define
 78 a zero-augmented probability density function (pdf) as follows:

$$f(y_{t,i} \mid \mu_{t,i}, \phi, \rho_{t,i}) = \begin{cases} \rho_{t,i}, & \text{if } y_{t,i} = 0, \\ (1 - \rho_{t,i})g(y_{t,i} \mid \mu_{t,i}, \phi), & \text{if } y_{t,i} > 0, \end{cases} \quad (1)$$

79 where $\rho_{t,i} = \Pr(Y_{t,i} = 0)$ is the probability of observing a zero density (which might in turn
 80 depend on observation effort or $\mu_{t,i}$); and $g(\cdot \mid \mu_{t,i}, \phi)$ is the pdf of a continuous probability
 81 distribution with expected value, or theoretical mean, $\mathbb{E}[Y_{t,i} \mid Y_{t,i} > 0] = \mu_{t,i}$ and additional
 82 parameter ϕ . This distribution represents the densities of the species when it is present.
 83 Popular choices such as the Log-Normal, Log-Logistic, and Gamma distributions are readily
 84 available in the package. We parametrize these three families of distributions in terms
 85 of their theoretical mean value to facilitate modeling (Ye et al., 2021). A side effect of
 86 such a parametrization is that the additional parameter, denoted ϕ , is not always readily
 87 interpretable. While this is a limitation, we prioritized being able to model the mean of a
 88 distribution over to easily interpreting its nuisance parameters.

89 2.1 Dynamic range models

90 While both DRMs and SDMs can relate environmental variables to zero-augmented densi-
91 ties (Equation (1)), DRMs use demographic processes to constrain the dynamics of density
92 across space and through time. Specifically, a DRM separates this observation model (en-
93 coded through the zero-augmented distribution) from an explicit process model. Underlying
94 biological mechanisms that drive species distributions are what inform the latter. This sepa-
95 ration enables the powerful integration of knowledge regarding species demography, dispersal,
96 and mechanistic interactions with environmental factors (Pagel and Schurr, 2012).

97 The assumptions of our DRM are placed on the conditional mean density $\mu_{t,i}$, with the
98 probability of absence remaining the same as in a typical zero-augmented SDM. In fact,
99 those assumptions can be interpreted as a biologically informed non-linear function of the
100 environmental variables. Specifically, we put biological constraints on the unobserved age-
101 structure behind the densities at a given time point and patch. Define $Y_{a,t,i}$ as a random
102 variable representing the unobserved density for individuals of age a , where $a \in \{1, \dots, A\}$.
103 We assume that if the species is absent (i.e., $Y_{t,i} = 0$), then $Y_{a,t,i} = 0$ for all a . We denote the
104 respective age-specific expected densities as $\lambda_{a,t,i} = \mathbb{E}[Y_{a,t,i} \mid Y_{t,i} > 0]$. Although we do not
105 observe $Y_{a,t,i}$, we assume $Y_{t,i} = \sum_a Y_{a,t,i}$. Consequently, by the linearity property of expected
106 values, we have

$$\mu_{t,i} = \sum_a \lambda_{a,t,i}. \quad (2)$$

107 Biological processes and additional assumptions are encoded through the expected age-
108 specific densities $\lambda_{a,t,i}$. In addition, we can allow for explicit relationships between the
109 mean density $\mu_{t,i}$ and $\rho_{t,i}$, as higher densities should decrease the probability of observing
110 zeros (Lambert, 1992; Yee, 2014).

111 Our implementation supports explicitly accounting for three key processes: recruitment,
112 survival, and movement. Each process is thoroughly described in the upcoming Sections.
113 The most basic model (when the user does not specify anything about the processes) does

114 not allow movement between spatial habitat patches and assumes recruitment and survival
 115 rates are constant across time and space. In addition, in this basic version, only the recruit-
 116 ment rate is estimated, while the survival rate is a constant, user-defined value. All model
 117 configurations require initialized age-specific densities, which can be derived from the total
 118 density, assumed mortality rates, or estimated as free parameters via the `est_init` toggle;
 119 for more details, see `vignette("init", "drmr")` in the R package.

120 2.1.1 Recruitment

121 We begin by defining the expected density for recruits at time t and patch i as:

$$\mathbb{E}[Y_{1,t,i}] = \lambda_{1,t,i} = \exp\{\psi\}, \quad (3)$$

122 where $\exp\{\psi\}$ represents the overall mean recruitment per unit of area. The assumption in
 123 Equation (3) is quite restrictive. We can obtain a more realistic model by replacing ψ with

$$\psi_{t,i} = \boldsymbol{\beta}_r^\top \mathbf{x}_{t,i}^{(r)}, \quad (4)$$

124 where $\mathbf{x}_{t,i}^{(r)}$ is a vector of environmental drivers associated to recruitment at time t and patch i ,
 125 $\boldsymbol{\beta}_r$ is a vector of corresponding regression coefficients. This depicts a log-linear relationship
 126 between recruitment and the environment. Gaussian relationships between recruitment and
 127 environmental conditions can be easily included by adding squared terms in $\mathbf{x}_{t,i}^{(r)}$.

128 2.1.2 Survival

129 In the proposed model, the expected density at age a , time t , and patch i evolves over time
 130 according to survival rates denoted $s_{a,t,i}$. Formally, we have

$$\mathbb{E}[Y_{a,t,i}] = \lambda_{a,t,i} = \lambda_{a-1,t-1,i} \cdot s_{a-1,t-1,i} \text{ for } a > 1. \quad (5)$$

131 As with recruitment, the survival rates may vary by patch i and time t :

$$\text{logit}(s_{a,t,i}) = \boldsymbol{\beta}_s^\top \mathbf{x}_{t,i}^{(s)}, \quad (6)$$

132 where $\mathbf{x}_{t,i}^{(s)}$ represents environmental drivers, which can be different from those affecting
133 recruitment, and $\boldsymbol{\beta}_s$ are associated regression coefficients. Note that, despite the age-specific
134 index a , the survival rates are constant across age-groups and, moreover, the logit link
135 function ensures the survival rates within the $[0, 1]$ interval.

136 External information can be incorporated into Equation (6) to model age-specific survival
137 rates. For example, data on other mortality sources, such as hunting, may be available
138 from other studies or wildlife management agencies (Urban et al., 2016). Another example
139 occurs in fisheries, which often have age-specific fishing rates (Hilborn and Walters, 2013).
140 Assuming $f_{a,t}$ represents an instantaneous rate of mortality for the age-group a at time t ,
141 Equation (6) can be updated as follows:

$$s_{a,t,i} = \text{logit}^{-1}\{\boldsymbol{\beta}_s^\top \mathbf{x}_{t,i}^{(s)}\} \exp\{-f_{a,t}\}, \quad (7)$$

142 where logit^{-1} denotes the inverse of the logit function. Importantly, when provided, the
143 relationship between the mortality rates $f_{a,t}$ and survival is assumed to be deterministic
144 instead of estimated.

145 The literature often shows that survival rates vary with age (Healy et al., 2019). For
146 mammals, age-specific mortality is available from published life-tables (Heppell et al., 2000).
147 Senescence, an inevitable and irreversible accumulation of damage with age in ecology, leads
148 to functional loss and thus reduced survival rates (Gaillard and Lemaître, 2020; Monaghan
149 et al., 2008). If age-specific survival rates are available from the literature, they can be easily
150 included in Equation (7) by using the negative log of these rates as $f_{a,t}$. When rates are
151 constant across time, users can simply repeat them for all time points.

152 **2.1.3 Movement**

153 Movement can substantially impact species densities and encodes a basic law of geogra-
 154 phy that similarity increases with proximity. Our package models this using a basic dif-
 155 fusion routine, which represents undirected movement away from an organism’s current
 156 location (Thorson et al., 2021). Denote P the total number of patches in the present study.
 157 For each age-group, we define a $P \times P$ movement matrix denoted \mathbf{M}_a . The element $\{i, j\}$
 158 in \mathbf{M}_a represents the probability that individuals of age a move from patch i at time $t - 1$
 159 to patch j at time t . Here, the movement matrix \mathbf{M}_a is derived from adjacency matrix \mathbf{A} ,
 160 which encodes connections between patches. In \mathbf{A} , the element $\{i, j\}$ is given by

$$\mathbf{A}_{ij} = \begin{cases} 1/N(i), & \text{if } i \sim j, \\ 0, & \text{otherwise,} \end{cases} \quad (8)$$

161 where $N(i)$ is the number of neighbors of patch i , and $i \sim j$ indicates that i and j are
 162 neighbors (i.e., share borders). In this way, spatial structure can easily be defined as one-
 163 dimensional, two-dimensional, or as more complex network structures.

164 The user must also indicate which age-groups can move. If an age group is not assumed
 165 to move, the movement matrix becomes the identity matrix. Given those inputs, we define ζ
 166 as the probability of individuals remaining in the same patch between two time points. The
 167 movement matrix is then constructed as:

$$\mathbf{M}_a = \zeta \mathbf{I}_P + (1 - \zeta) \mathbf{A}, \quad (9)$$

168 where \mathbf{I}_P is a $P \times P$ identity matrix. In other words, individuals that move have equal
 169 probability of moving to any of the neighboring patches.

170 Once a movement matrix is defined, we adjust the age-specific expected densities accord-
 171 ingly. Let $\boldsymbol{\lambda}_{a,t} = [\lambda_{a,t,1}, \dots, \lambda_{a,t,P}]^\top$ be a vector of length P (number of patches) representing

172 the expected densities of age a at time t for every patch after survival and before movement.
173 After movement, the expected density is:

$$\tilde{\lambda}_{a,t,\cdot} = \mathbf{M}_a \lambda_{a-1,t-1,\cdot} \quad (10)$$

174 Next, $\lambda_{a-1,t-1,i}$ in Equation (5) is replaced by $\tilde{\lambda}_{a-1,t-1,i}$, where the latter represents the i -th
175 element of $\tilde{\lambda}_{a,t,\cdot}$.

176 2.1.4 Patch, spatial, and temporal dependence

177 The models presented thus far assume that, after accounting for measured environmental
178 covariates and dispersal, the densities in different patches and at different times are inde-
179 pendent. This assumption is often violated in ecological data, as unmeasured factors can
180 create correlations across space and time. To address this, `drmr` allows for the inclusion of
181 random effects to model this residual dependence. These effects can be incorporated into
182 the sub-models for recruitment (Equation (4)), survival (Equation (6)), or the mean density
183 directly (Equation (2)).

184 The package supports three distinct random effect structures. The simplest structure
185 uses independent and identically distributed (IID) random effects to introduce a patch-
186 specific intercept for a given process. This accounts for time-invariant local factors not
187 captured by the environmental drivers. These effects are assumed to be independent across
188 all patches, with each patch's effect being drawn from a common distribution, effectively
189 shrinking estimates toward a global mean.

190 When nearby patches are expected to be more similar than distant ones due to unmea-
191 sured, spatially structured variables (e.g., [Paradinas et al., 2023](#)), a spatial random effect
192 can be used. This structure assumes that the random effect for a given patch is correlated
193 with the effects in its neighboring patches. `drmr` implements this using an intrinsic Condi-
194 tional Autoregressive ([Besag et al., 1991](#); [Morris et al., 2019](#), ICAR) model, which shrinks

195 patch-specific effects towards a local, rather than global, mean.

196 To account for serial autocorrelation in population dynamics that is common to all
197 patches and not explained by the covariates, a temporal random effect can be added. The
198 package implements this as a first-order autoregressive (AR(1)) process, which models the
199 dependency between observations at time t and time $t - 1$. By incorporating these random
200 effects, users can build more realistic models that better capture the complex sources of
201 variation inherent in spatio-temporal ecological data.

202 **2.2 Bayesian inference**

203 To allow Bayesian inference, we specify Normal priors for the regression coefficients (e.g., β_r
204 and β_s), a Gamma prior for the nuisance parameter (ϕ), and a Beta prior for the movement
205 parameter (ζ). When random effects are included, we place Normal priors on the log-
206 transformed standard deviation of those effects. For the autocorrelation parameter, denoted
207 α , in the AR(1) structure, we use a Beta prior because negative temporal autocorrelation
208 is rare in practice. Further details on prior specifications and default hyperparameters are
209 available in a package vignette (`vignette("ppt", "drmr")`). We use the No-U-Turn Sam-
210 pler (NUTS) MCMC algorithm, implemented in Stan (Homan and Gelman, 2014), to sample
211 from the joint posterior distribution. MCMC initialization is performed using either Stan's
212 default, drawing from priors, or the Pathfinder algorithm (Zhang et al., 2022). Forecasts in-
213 corporating parameter uncertainty are generated by sampling from the posterior predictive
214 distribution. We report posterior medians as point estimates and symmetric 90% credible
215 intervals (posterior percentiles) for uncertainty quantification unless otherwise stated.

216 **3 The drmr R package**

217 Given the model structure explained so far, the `drmr` package offers functions to facilitate
218 data analyses based on DRMs. The `fit_drm` has an analogous counterpart for GLM-based

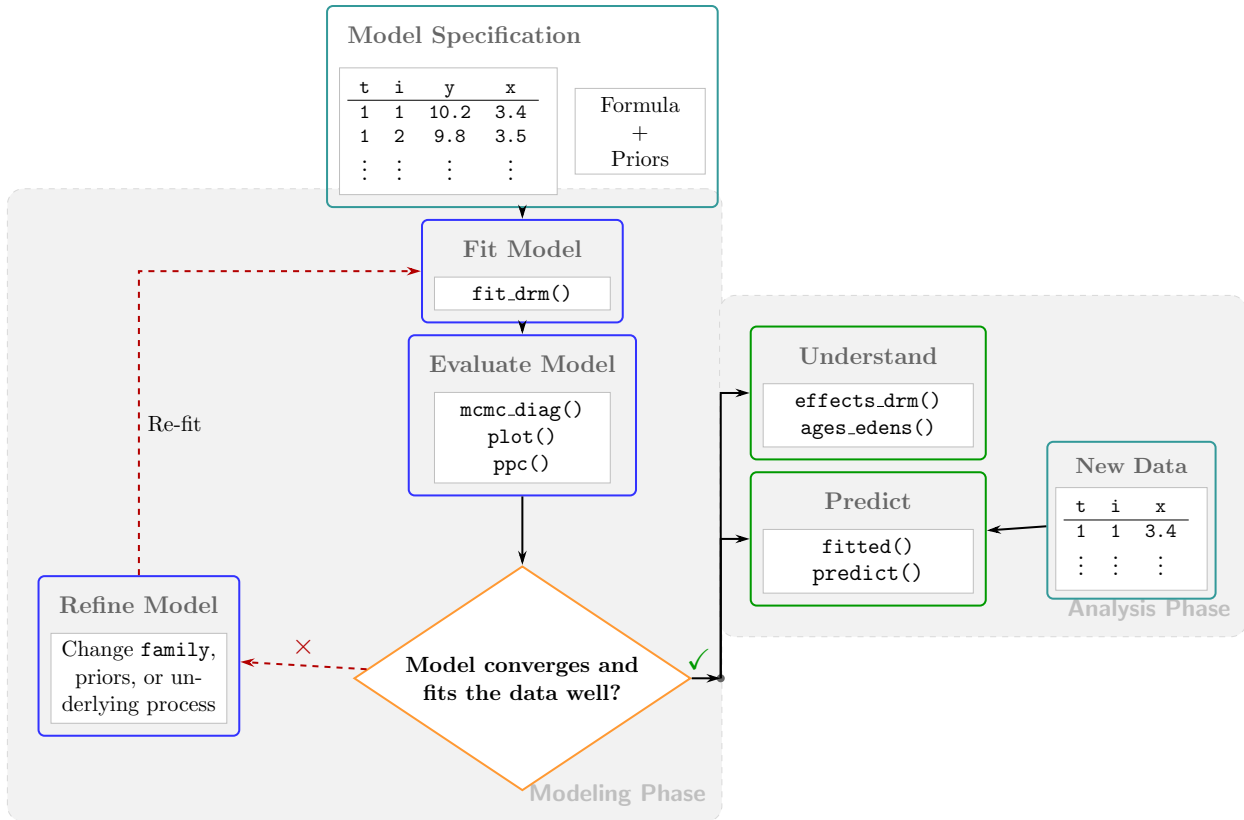


Figure 1: `drmr` modeling workflow. The diagram outlines the iterative analytical process, highlighting key R functions and expected input data formats at each stage. In the example datasets presented along the diagram, t represents the time column, i is the patch column, y is the response variable (e.g., density), and x stands for an environmental driver.

219 SDMs (`fit_sdm`), enabling consistent fitting and fair comparison across model types using the
 220 same data. These core functions are `Stan` wrappers that prepare data and run pre-compiled
 221 models bundled with the package. Their outputs have their own class (`drmrmodels`) for which
 222 we provide `print`, `summary`, `update` and `draws` methods. The latter is used to easily retrieve
 223 samples from the parameters' posterior distributions. A suggested workflow is presented in
 224 Fig. 1, along with some of the most important functions available in the package.

225 The following example demonstrates a minimal reproducible workflow using `drmr`'s de-
 226 fault priors and assuming no movement between patches. The `summary` method outputs the
 227 parameters along with the posterior mean, standard deviation, and percentiles (5%, 50%
 228 and 95%, by default) based on the samples from posterior distributions.

```

## Load the package and example data
library(drmr)
data(sum_fl)

## Creating number of individuals per unit of area to be the response variable
sum_fl <- transform(sum_fl, dens = y / area_km2)

fit <- fit_drm(.data = sum_fl,      ## dataset
              y_col = "dens",      ## column representing response variable
              time_col = "year",   ## column representing time variable
              site_col = "patch",  ## column representing patch/site
              seed = 2026,         ## seed for reproducibility
              ## recruitment has an intercept and a coefficient for
              ## surface temperature (stemp)
              formula_rec = ~ 1 + stemp)

summary(fit)
#> Summary of ADRM Fit
#>
#> Estimates:
#> # A tibble: 5 × 7
#>   variable description          mean    sd    q5    q50    q95
#>   <chr>    <chr>                <dbl> <dbl> <dbl> <dbl> <dbl>
#> 1 beta_t[1] zero-infl: (Intercept) -4.32  1.13  -5.94  -4.48  -2.07
#> 2 beta_r[1] rec: (Intercept)      -9.03  0.617 -9.86  -9.12  -7.88
#> 3 beta_r[2] rec: stemp             0.112 0.0301 0.0562 0.116 0.152
#> 4 xi[1]    Relationship between zeros and density -0.578 0.174 -0.821 -0.603 -0.230
#> 5 phi[1]   Dispersion parameter          0.820 0.0668 0.715 0.817 0.932

```

229 To use `drmr`, the input data must follow a “long” format where each row corresponds to a
230 specific patch and time point. The dataset must be spatio-temporally complete, containing
231 all patches for every time step across the study period. While missing values are permitted
232 in the response variable and are automatically estimated by the model, information on
233 environmental drivers must be provided for all patch-time combinations. This ensures that
234 the demographic processes underlying the DRM can be modeled continuously throughout

235 the study duration, even in the absence of species observations.

236 Running the models provided by the package relies on a small number of critical de-
237 pendencies. The primary dependency is `CmdStan` (version ≥ 2.36). As the computational
238 backbone, `CmdStan` is used via the `instantiate` interface (Landau, 2024) to pre-compile the
239 package’s `Stan` models during installation. Please note that `CmdStan` versions prior to 2.36
240 are unsupported and may lead to unexpected behavior. Another key dependency is the `sf`
241 package (Pebesma, 2018), primarily used to generate the adjacency matrix required for the
242 DRM’s movement component. Finally, for availability, the package is hosted on [GitHub](#).

243 To accommodate varying computational requirements and research stages, `drmr` sup-
244 ports several inference algorithms beyond the default NUTS sampler. Users can utilize the
245 Pathfinder algorithm (Zhang et al., 2022), Laplace approximation, or Automatic Differen-
246 tiation Variational Inference (Kucukelbir et al., 2017, ADVI) to obtain faster, approximate
247 posterior estimates. These alternatives are implemented in `Stan` and are particularly effec-
248 tive for rapid model prototyping, initial hypothesis screening, or providing robust starting
249 values for a final MCMC run. While these methods offer significant speed advantages, we
250 recommend the default MCMC-based inference for final results to ensure rigorous uncer-
251 tainty quantification. A comparison of these algorithms and their performance trade-offs is
252 available in the package documentation (`vignette("algos", "drmr")`).

253 Different assumptions about the DRM can be conveniently modified through a series of
254 “toggles”. The toggles allow users to turn some of the features described in Section 2.1 on or
255 off. This is achieved by passing a named list as an argument called `.toggles` to the `fit_drm`
256 function. To turn a feature on, we make the respective list element equal to 1, while to turn
257 it off, we make it equal to 0. A complete list of those toggles and their respective default
258 values is displayed in Table 2. Alternatively, one can consult the default toggles by running
259 `drmr::default_toggles()`. Note that, if nothing is provided, the default values are used.
260 If we provide a list with a single named element, say `list(movement = 1)`, the `movement`
261 feature (e.g., Section 2.1.3) will be turned on, while the other features will be kept at their

Table 2: Toggles associated with specific model features, their descriptions, and default states. For the last three toggles, the options are "none" (no random effect), "rec" (random effect for recruitment), "surv" (random effect for survival), and "dens" (random effect for density).

Toggle	Description	Default State
<code>rho_mu</code>	Explicitly relates density (μ) and the probability of observing a zero (ρ).	On
<code>cloglog</code>	Use the complementary log-log (cloglog) link function for ρ . If off, the logistic link function is used.	Off
<code>movement</code>	Enable the movement routine as described in the paper.	Off
<code>est_surv</code>	Estimate survival probabilities within the model.	On
<code>est_init</code>	Estimate initial values.	Off
<code>minit</code>	Initial values driven by mortality rates.	Off
<code>iid_re</code>	Include an IID Random effect.	"none"
<code>ar_re</code>	Include an AR(1) random effect.	"none"
<code>sp_re</code>	Include an ICAR random effect.	"none"

262 default values.

263 Complementary tools for diagnosing and understanding the results are also available.
 264 The functions `mcmc_diag` provides statistics such as the split- \hat{R} , the bulk and tail effective
 265 sample size (Vehtari et al., 2021, ESS). Although these statistics alone cannot establish
 266 convergence, some rules of thumb are common. For instance, $\hat{R} < 1.01$, bulk-ESS > 400
 267 and tail-ESS > 400 provide reasonable evidence of convergence (Vehtari et al., 2021). In
 268 addition, the trace-plots available from calling `plot` on the output of our `fit_*` functions can
 269 aid the process of assessing the convergence. Lastly, the `ppc` function provides a posterior
 270 predictive check (Gabry et al., 2019, PPC), where the empirical density of the data can be
 271 compared to that of the induced posterior predictive distributions. In other words, it shows
 272 how well the model fits to the data.

273 After establishing model convergence, a suite of post-estimation functions allows for
 274 interpreting the relationships between environmental drivers and demographic processes.
 275 Specifically, the `effects_drm` function extracts the estimated impact of a chosen covariate on

276 a target process (e.g., recruitment or survival, specified as "rec" or "surv"). To visualize the
277 estimated population structure, `ages_edens` extracts age-specific latent densities, whereas
278 `fitted` and `predict` return in-sample and out-of-sample predictions, respectively. In the
279 latter two, a `type` parameter allows for choosing between the following types of predictions: (i)
280 the posterior predictive distribution of $Y_{t,i}$ (accounting for data variability and detectability);
281 (ii) its mean, $(1 - \rho_{t,i})\mu_{t,i}$ (accounting for detectability but removing observation error); or
282 (iii) the latent densities, $\mu_{t,i}$ (excluding both variation sources to reflect only the assumed
283 population dynamics). Finally, `log_lik` integrates with the `loo` package to compute the
284 Leave-One-Out Information Criterion (Vehtari et al., 2017, LOOIC), which facilitates model
285 comparison.

286 4 Case studies

287 The features of the package are best illustrated through the analysis of real datasets. To
288 this end, we showcase its functionalities using data from two distinct species: the summer
289 flounder (*Paralichthys dentatus*) and the red-bellied woodpecker (*Melanerpes carolinus*).
290 Despite the ecological differences between these species, our interface easily accommodates
291 models with varying assumptions. For both case studies, we fit two distinct DRMs: one
292 with environment-dependent recruitment and another with environment-dependent survival.
293 For the summer flounder, we extend this by fitting a third model that incorporates both
294 environment-dependent recruitment and survival, while also accounting for known fishing
295 mortality. Across all case studies, the DRMs assume a Gamma probability density function
296 for population densities, allow for movement, and include a temporal autoregressive term on
297 recruitment. Finally, we emphasize that these case studies are designed strictly to demon-
298 strate the versatility, workflow, and application of the package. They are not intended to
299 serve as comprehensive ecological evaluations or definitive performance comparisons against
300 existing models.

301 In each case, we compare the models based on out-of-sample predictions. Specifically, we
302 reserved the last five years of data and assessed point prediction accuracy with root mean
303 square error (RMSE). To assess interval predictions, we used the interval score ([Gneiting and](#)
304 [Raftery, 2007](#), IS). The IS penalizes intervals based on their width and whether they contain
305 the true observation. Lower RMSE and IS values indicate better model performance.

306 4.1 Summer flounder

307 DRMs have been previously developed and evaluated for summer flounder ([Fredston et al.,](#)
308 [2025](#)). Here, we demonstrate how to use the package using a somewhat different model
309 structure from [Fredston et al. \(2025\)](#) but the same dataset: scientific bottom trawl surveys
310 in the United States of America (USA) from 1972-2016 ([Forrest et al., 2020](#)). The original
311 sampling unit for the survey consists of a “haul”, an event during which a fishing net is towed
312 along the seafloor. The haul data was aggregated across 10 patches along the northeast coast,
313 each with 1° latitude in height but varying width. The response variable was the number of
314 fish caught per unit of area. For convenience and reproducibility, this processed dataset is
315 included with the package. Users can view its documentation by running `help("sum_fl",`
316 `package = "drmr")`.

317 In our first model, we set the logit of probability of absence as a linear function of
318 the number of hauls (`c_hauls`) and the underlying theoretical density ($\mu_{t,i}$). The latter is
319 controlled by the `rho_mu` toggle. In addition, we establish a quadratic relationship between
320 log recruitment and seawater surface temperature (SST; `stemp`), which approximates a bell-
321 shaped curve once exponentiated. Those functional relationships are easily modified through
322 a formula syntax. We additionally assume an AR(1) effect for recruitment. The syntax to
323 fit this model is as follows:

```
## load package and data
library(drmr)
data(sum_fl)
```

```

## we omit the code to split the data into train and test here.
## The full script is available on GitHub

drm_rec <-

  fit_drm(.data = dat_train, ## a data.frame
    y_col = "dens", ## column for the response
    time_col = "year", ## column for time
    site_col = "patch", ## column for site
    family = "gamma", ## non-zero densities' pdf family
    seed = 202505, ## seed for reproducibility
    ## formula for the probability of absence
    formula_zero = ~ 1 + c_hauls,
    ## recruitment as a function of
    ## sea surface temperature (stemp)
    formula_rec = ~ 1 + c_stemp + I(c_stemp * c_stemp),
    ## formula for survival (intercept only)
    formula_surv = ~ 1,
    ## f_{a, t} from Equation (6)
    ## In this case, we input it as a matrix with "number of ages" rows
    ## and "number of time points" columns.
    f_mort = f_train,
    n_ages = NROW(f_train),
    ## A matrix from Equations (7) and (8)
    adj_mat = adj_mat,
    ages_movement = c(0, 0, ## ages not allowed to move
      rep(1, 12), ## ages allowed to move
      0, 0), ## ages not allowed to move
    .toggles = list(rho_mu = 1, ## relates density to probability
      ## of absence
      ## (0 is the default and turns it off)
    ar_re = "rec", ## AR(1) term for recruitment
      ## ("dens" for density,
      ## "surv" for survival,
      ## "none" is the default includes no AR(1))

```

```

movement = 1, ## uses movement routine from Equation (8)
            ## (0 is the default)
est_surv = 1, ## Estimate the survival rates
            ## (0 is the default)
minit = 1), ## Uses mortality to estimate the initial
            ## age-classes in the first years of study
            ## (0 is the default)

## some priors hyperparameters.
.priors = list(pr_alpha_a = 4.2, pr_alpha_b = 5.8,
              pr_zeta_a = 7, pr_zeta_b = 3),
## algorithm for inference. "nuts" is the default (MCMC)
## for other options see ?fit_drm
algorithm = "nuts",
## arguments to be passed to the inference algorithm.
## The default for nuts is to run 4 chains sequentially.
## here we are specifying to run 4 chains in parallel.
## The default arguments can be inspected by
## running: default_nuts()
algo_args = list(parallel_chains = 4))

```

324 The priors were set such that prior probability of remaining in the same site is 0.7, while the
325 prior temporal autocorrelation is 0.42. The former is arbitrary but biologically meaningful,
326 while the latter is based on estimates from the fisheries literature ([Johnson et al., 2016](#), e.g.).

327 Quick model diagnostics are obtained as follows:

```

mcmc_diag(drm_rec) |>
  print() |>
  summary()
#> # A tibble: 11 × 4
#>   variable      rhat ess_bulk ess_tail
#>   <chr>        <dbl> <dbl> <dbl>
#> 1 beta_t[1]    1.00  4253.  3200.
#> 2 beta_t[2]    1.00  5719.  2527.
#> 3 beta_r[1]    1.00  4246.  2852.

```

```

#> 4 beta_r[2]      1.00    5296.    3226.
#> 5 beta_r[3]      1.00    5543.    3196.
#> 6 xi[1]          1.00    4376.    2905.
#> 7 phi[1]         1.00    7562.    3293.
#> 8 zeta[1]        1.00    5280.    2793.
#> 9 beta_s[1,1]    1.00    4144.    3007.
#> 10 alpha[1]      1.00    5448.    3284.
#> 11 sigma_t[1]    1.00    4077.    3355.
#> No issues detected by the MCMC diagnostics.

```

328 The first column represents the model parameter, with the three remaining columns high-
329 lighting three different convergence diagnostics' metrics. The `summary` call quickly scan
330 the rules of thumb to check if there is any evidence of convergence issues. By running
331 `plot(drm_rec)` one can quickly inspect the trace-plots for each model parameter. Since
332 there is no evidence of any convergence issues, we can inspect the parameter estimates using
333 the `summary` function:

```

summary(drm_rec)
#> Summary of ADRM Fit
#>
#> Estimates:
#> # A tibble: 11 × 7
#>   variable      description      mean      sd      q5      q50      q95
#>   <chr>         <chr>          <dbl>    <dbl> <dbl> <dbl> <dbl>
#> 1 beta_t[1]    zero-infl: (Intercept) -5.35  0.541  -6.27  -5.33  -4.50
#> 2 beta_t[2]    zero-infl: c_hauls    -0.0549 0.0161 -0.0821 -0.0545 -0.0295
#> 3 beta_r[1]    rec: (Intercept)     -2.57  0.181  -2.85  -2.58  -2.26
#> 4 beta_r[2]    rec: c_stemp          0.270  0.0276  0.226  0.269  0.316
#> 5 beta_r[3]    rec: I(c_stemp * c_stemp) -0.0547 0.00680 -0.0663 -0.0545 -0.0438
#> 6 xi[1]       Relationship between zeros and density -1.64  0.205  -1.99  -1.63  -1.33
#> 7 phi[1]      Dispersion parameter   1.45  0.142  1.22  1.45  1.69
#> 8 zeta[1]     Prob. of remaining at the current patch 0.705  0.125  0.477  0.716  0.891
#> 9 beta_s[1,1] surv: (Intercept)     1.48  0.564  0.604  1.44  2.46

```

```

#> 10 alpha[1]    Temporal autocorrelation          0.477 0.152    0.223 0.478 0.723
#> 11 sigma_t[1] Temporal random effect std. dev. 0.171 0.0457 0.108 0.166 0.253

```

334 In this case, the standard output contains the parameters (**variables**), followed by their
335 description, and some summary statistics from their posterior distribution.

336 An interesting competing hypothesis is that seawater bottom temperature (SBT; **btemp**)
337 drives the species' survival rates. We can update the model to take that into account using
338 the **update** method:

```

drm_surv <-
  update(drm_rec,
        formula_rec = ~ 1,
        ## survival as a function of
        ## sea bottom temperature
        formula_surv = ~ 1 + c_btemp + I(c_btemp * c_btemp))

```

339 When using the **update** method, only the provided arguments are modified from the model
340 fit being updated (**drm_rec**, in this case). We can use this method to fit a model under the
341 hypothesis that both demographic processes are influenced by the environment:

```

drm_rs <-
  update(drm_rec,
        ## survival as a function of
        ## sea bottom temperature
        formula_surv = ~ 1 + c_btemp + I(c_btemp * c_btemp))

```

342 Notice that, in this case, we retain the original relationship between recruitment and SST.

343 The **predict** method enables us to seamlessly obtain the out-of-sample predictions. This
344 function always needs at least three arguments, the output of a **fit_drm** call, a dataset with
345 the patches, time-points and environmental variables where we seek to obtain predictions,
346 and a seed for random number generation. When we estimate survival, we need to pass
347 the data from the last year used for model fitting to the function as well. The code below

348 illustrates how to use this function with the outputs of the DRMs fitted in this Section. Im-
349 portantly, the argument `f_test` (which represents $f_{a,t}$ associated to `new_data`) is optional and
350 should only be provided when external mortality information is available (see Equation (7)).

```
proj_rec <- predict(drm = drm_rec,  
                  new_data = dat_test,  
                  past_data = filter(dat_train,  
                                     year == max(year)),  
                  ## `f_test` is similar to `f_train`. The difference  
                  ## is that the number of columns coincides with the  
                  ## number of time points where we wish to make predictions.  
                  f_test = f_test,  
                  seed = 125,  
                  cores = 4)
```

```
proj_surv <- predict(drm = drm_surv,  
                   new_data = dat_test,  
                   past_data = filter(dat_train,  
                                       year == max(year)),  
                   seed = 125,  
                   f_test = f_test,  
                   cores = 4)
```

```
proj_rs <- predict(drm = drm_rs,  
                 new_data = dat_test,  
                 past_data = filter(dat_train,  
                                     year == max(year)),  
                 seed = 125,  
                 f_test = f_test,  
                 cores = 4)
```

351 The density estimates from the DRM appear to capture more of the population growth
352 in the northern patches, both in the fitted and the out-of-sample forecasts (Fig. 2). In
353 Table 3, we present the predictive skill metrics for each model, sorted by the RMSE. The

Table 3: Predictive skill for the summer flounder models. Out-of-sample indicates whether the predictions are in- or out-of-sample. Model distinguish between the fitted model by highlighting which demographic processes (Rec, Surv) depend on the environment. RMSE is the root mean square error of prediction, and IS is the interval score.

Out-of-sample	Model	RMSE	IS (90%)
No	Rec + Surv	0.02	0.36
	Rec	0.02	0.41
	Surv	0.02	0.47
Yes	Rec + Surv	0.11	1.61
	Rec	0.12	1.66
	Surv	0.12	1.97

354 results suggest that the DRM (rec-surv) does better both for in-sample and out-of-sample
 355 predictions. In terms of interval predictions (assessed using the IS), all models do better
 356 in-sample than out-of-sample, as expected.

357 The value from DRMs extends beyond simply better predictive performance. These
 358 models also allow researchers to examine how environmental conditions affect demographic
 359 processes. For example, the panel in Fig. 3 depicts the estimated relationship between
 360 recruitment and SST and between survival and SST from the DRM that relates both re-
 361 cruitment and survival to environmental variables. Those curves, can be easily obtained by
 362 running:

```

drm_effects(drm_rs,                ## output form fit_drm
            process = "rec",        ## the demographic process we wish to analyze
            variable = "c_stemp") |> ## an environmental variable

plot()

drm_effects(drm_rs,
            process = "surv",
            variable = "c_btemp") |>

plot()

```

363 In addition to the curves, the DRM (rec) model suggests that recruitment is maximized
 364 with a SST of 21.3°C (90% CI: 20.6 to 22.5). On the other hand, the DRM (surv) models
 365 suggests that the optimal SBT for survival is near 13.7°C (90% CI: 13.0 to 14.5).

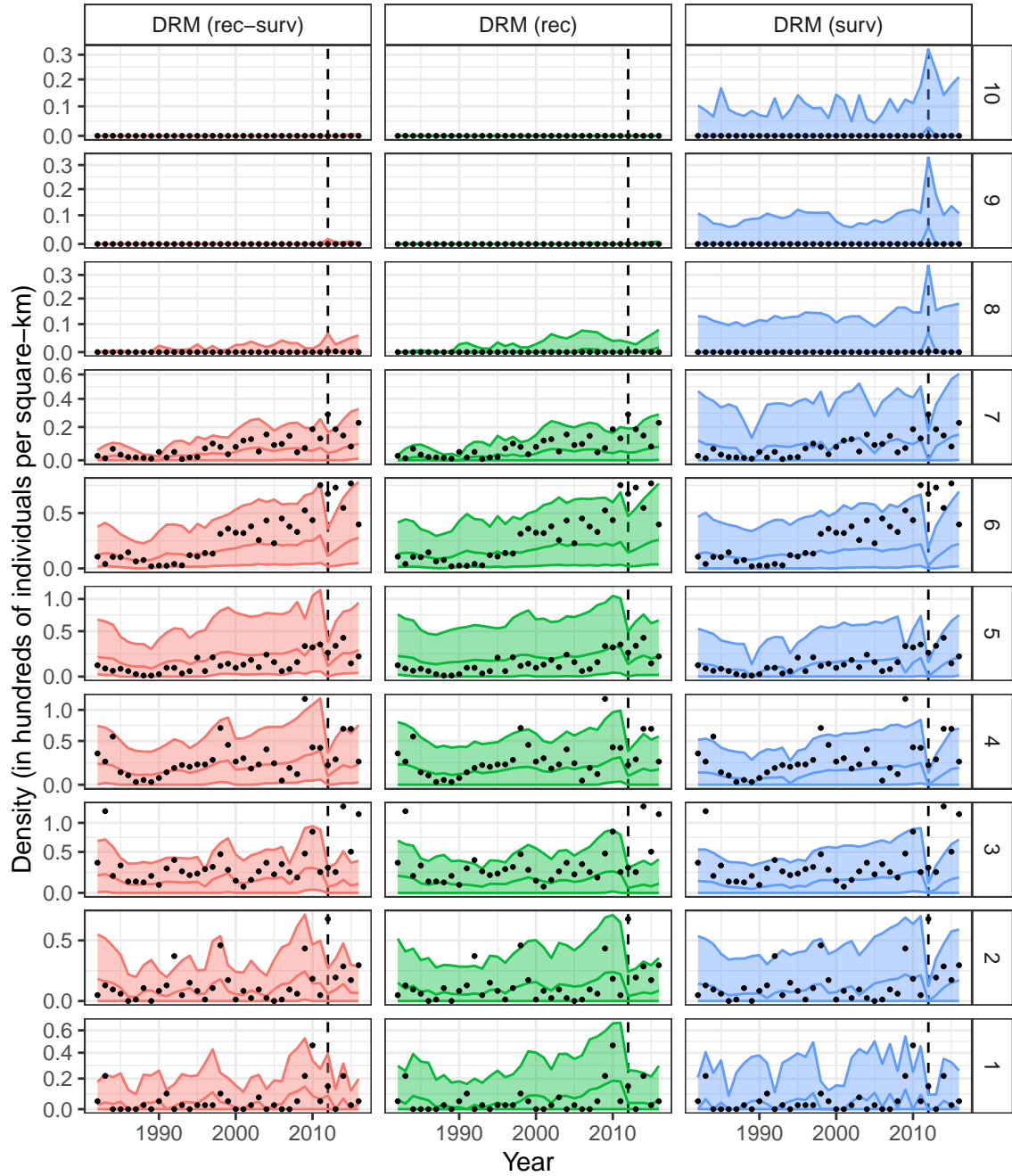


Figure 2: Predicted summer flounder densities per patch in the training years (left of the dashed line) and in the out-of-sample testing years (right of the dashed line). Colored lines show the posterior median, shaded area shows the 90% prediction interval (PI), and black dots show the observations. Patches are arranged from 10 (northernmost) to 1 (southernmost). The columns show results from a DRM with environmentally linked recruitment and survival (rec-surv), a DRM with environmentally linked recruitment (rec), and a DRM with environmentally linked survival (surv).

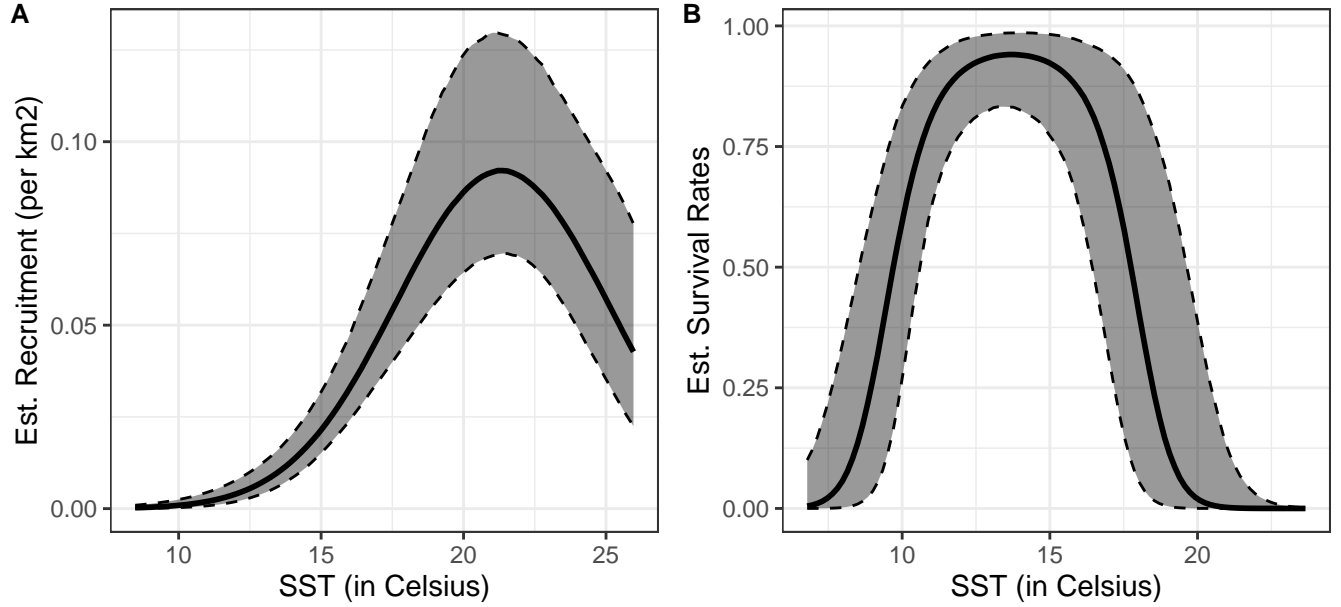


Figure 3: Panel containing the estimated relationship for summer flounder between recruitment and seawater surface temperature (SST) for the DRM (rec) model on the left hand side, and the relationship between survival rates and seawater bottom temperature (SBT) in the DRM (surv) model on the right hand side. The plots show the posterior median and 90% credible interval (CI).

366 4.2 Red-bellied woodpecker

367 To demonstrate the package’s flexibility, we apply the same models to the red-bellied wood-
 368 pecker, which is a resident bird species distributed throughout the eastern United States (Shack-
 369 elford et al., 2000). We obtained abundance data from the North American Breeding Bird
 370 Survey (Ziolkowski Jr et al., 2024, BBS) via the `bbsBayes2` package (Edwards et al., 2024).
 371 This survey’s data are collected along thousands of randomly established roadside routes
 372 throughout the continent. For the analysis, we used data from 1980 to 2019 aggregated
 373 into 273×273 km grids. The grids were then clipped to the continental USA, resulting in
 374 variable cell areas, particularly along the coast. Air temperature data from CHELSA (Karger
 375 et al., 2017; Brun et al., 2022) were aggregated to the same spatial resolution.

376 The code used to fit the models and generate predictions is essentially identical to the
 377 previous case study. Thus, it is omitted here but fully available on [GitHub](#). The environment-

378 dependent recruitment and survival versions of the model were set as a quadratic function
 379 of air temperature. For both models, the probability of absence was set as a function of
 380 the number of routes and theoretical density ($\mu_{t,i}$). Taking advantage of the larger dataset
 381 in this example, we also incorporated an ICAR random effect into the linear predictor of
 382 survival (Equation (6)). Movement was allowed among adjacent grid cells.

Table 4: Predictive skill for the red bellied woodpecker models. Out-of-sample indicates whether the predictions are in- or out-of-sample. Model distinguish between the fitted model by highlighting which demographic processes (Rec, Surv) depend on the environment. RMSE is the root mean square error of prediction, and IS is the interval score.

Out-of-sample	Model	RMSE	IS (90%)
No	Rec	0.03	0.62
	Surv	0.03	0.59
Yes	Rec	0.08	0.79
	Surv	0.11	1.26

383 The model results (Table 4) suggest the environment-dependent recruitment model de-
 384 livers a better out-of-sampel predictive performance. The model considering environment-
 385 dependent survival performed well regarding in-sample predictions, but its the environment-
 386 dependent recruitment counterpart provides better out-of-sample predictions (both in terms
 387 of RMSE and IS). The results indicated that recruitment peaked at an air temperature
 388 of 16.6°C (90% CI: 16.3 to 17.0), while maximum survival occurred at a similar temperature
 389 of 15.2°C (90% CI: 15.1 to 15.3).

390 5 Discussion

391 The `drmr` package offers an accessible framework for implementing DRMs, addressing the
 392 limitations of traditional correlative SDMs and the complexity barrier of DRMs. It provides a
 393 user-friendly interface for building, fitting, evaluating, and projecting age-structured DRMs,
 394 allowing researchers to consider movement and to explicitly link environmental drivers to
 395 demographic processes, like recruitment and survival, that drive shifts in species geographic
 396 distributions. Our fish and bird case studies demonstrated `drmr`'s utility in comparing dif-

397 ferent model structures. These examples highlight the package’s value for generating more
398 robust ecological forecasts of species on the move. Key package features include functions for
399 fitting models, generating predictions that account for parameter uncertainty, and visualizing
400 estimated process-environment relationships.

401 `drmr` distinguishes itself within ecological modeling software by focusing on environmentally-
402 driven and spatially explicit population demography inferred from spatio-temporal obser-
403 vations. This contrasts with other tools addressing related questions. `NicheMapR` excels
404 at mechanistic modeling of individual organismal performance based on microclimate and
405 metabolic theory, and it is parameterized extensively based on prior knowledge (Kearney
406 et al., 2021). Virtual species platforms like `RangeShifter` (Bocedi et al., 2021; Malchow
407 et al., 2021) and `rangr` (Markowska et al., 2025) simulate the spatial, demographic, and/or
408 evolutionary dynamics of an imaginary species across space based on user-specified assump-
409 tions about environmental responses and other parameters. By estimating the parameters of
410 mechanistic, spatial population dynamics models from species observations, `drmr` provides
411 an important tool for species that lack the detailed prior knowledge that could otherwise
412 parameterize a virtual species model (while recognizing that virtual species models can be
413 calibrated against data in some cases, e.g., Malchow et al. (2024) and `poems`). In this way,
414 `drmr` combines the ease of fitting SDMs with the mechanistic detail of virtual species models,
415 bridging an important gap between the two approaches. By allowing alternative models to
416 be compared against data, `drmr` also opens the door to testing mechanistic hypotheses about
417 the processes and environmental factors driving range shifts.

418 The applications of `drmr` are broad, extending to any species where spatio-temporal
419 abundance or density data are available and where understanding the demographic mecha-
420 nisms of environmentally driven geographic distribution changes are important. Given the
421 large fraction of Earth’s biodiversity now shifting to new locations, we expect the application
422 opportunities are many (Pecl et al., 2017). Birds, trees, mammals, insects, and fishes are
423 among the taxonomic groups with particularly extensive observations (Sullivan et al., 2009;

424 [Sauer et al., 2003](#); [Conn et al., 2015](#); [Maureaud et al., 2024](#); [Serra-Diaz et al., 2016](#)). Beyond
425 fundamental knowledge about ecological responses to environmental change, improved under-
426 standing and projection of range shifts can provide insights relevant for spatial conservation
427 planning, natural resource management, evaluation of alternative management strategies,
428 species reintroductions, governance planning for transboundary range shifts ([Pinsky et al.,](#)
429 [2018](#)), and other areas where population-level viability across landscapes is important ([Urban](#)
430 [et al., 2016](#)).

431 Despite its utility, `drmr` also has limitations. Currently, it models continuous densities
432 rather than discrete counts, mainly because `Stan` does not support latent discrete variables
433 previously used in this class of models (e.g., [Pagel and Schurr, 2012](#)). The implemented
434 movement routine is simplified, assuming diffusion among neighbors, although the package
435 structure allows for future expansion. In addition, survival rates are modeled as constant
436 across age classes unless external age-specific data (e.g., harvest rate-at-age) are provided.
437 The current implementation of temporal random effects is limited to an AR(1) process.
438 Furthermore, increasing model complexity, such as adding movement or more age classes,
439 naturally increases computational time.

440 In future developments, we aim to enhance `drmr`'s flexibility and realism. Planned ex-
441 tensions include incorporating more sophisticated movement routines that vary with time,
442 patch, age, or environmental conditions (e.g., [Thorson et al., 2021](#)); allowing more flexible
443 process-environment relationships using basis functions (as in generalized additive models);
444 and adding alternative population dynamics like negative density-dependent recruitment
445 via Ricker or Beverton-Holt stock-recruit functions ([Hilborn and Walters, 2013](#)). Provid-
446 ing support for age- or length-composition data and exploring options for handling count
447 data directly are also key goals. These enhancements will continue to broaden the scope for
448 applying mechanistic DRMs across diverse ecological systems.

449 Code and Data Availability

450 The `drmr` package is open-source and available under the GPL-3 license. The source code,
451 documentation, and all data used in the case studies will be released on GitHub upon
452 acceptance.

453 References

454 Besag, J., J. York, and A. Mollié (1991). Bayesian image restoration, with two applications
455 in spatial statistics. *Annals of the Institute of Statistical Mathematics* 43(1), 1–20.

456 Bocedi, G., S. C. F. Palmer, A.-K. Malchow, D. Zurell, K. Watts, and J. M. J. Travis
457 (2021). Rangesifter 2.0: an extended and enhanced platform for modelling spatial eco-
458 evolutionary dynamics and species’ responses to environmental changes. *Ecography* 44(10),
459 1453–1462.

460 Brun, P., N. E. Zimmermann, C. Hari, L. Pellissier, and D. N. Karger (2022). CHELSA-
461 BIOCLIM+ a novel set of global climate-related predictors at kilometre-resolution.

462 Conn, P. B., D. S. Johnson, J. M. V. Hoef, M. B. Hooten, J. M. London, and P. L. Boveng
463 (2015). Using spatiotemporal statistical models to estimate animal abundance and infer
464 ecological dynamics from survey counts. *Ecological Monographs* 85(2), 235–252.

465 Edwards, B. P. M., A. C. Smith, and S. LaZerte (2024). bbsBayes2: Hierarchical Bayesian
466 analysis of North American BBS data. version 1.1.2.1.

467 Engler, R. and A. Guisan (2009). MigClim: Predicting plant distribution and dispersal in a
468 changing climate. *Diversity and distributions* 15(4), 590–601.

469 Evans, M. R. and A. Moustakas (2016). A comparison between data requirements and
470 availability for calibrating predictive ecological models for lowland uk woodlands: learning
471 new tricks from old trees. *Ecology and Evolution* 6(14), 4812–4822.

472 Fallert, S., L. Li, and J. S. Cabral (2025). metaRange: A framework to build mechanistic
473 range models. *Methods in Ecology and Evolution* 16(1), 49–56.

474 Fordham, D. A., S. Haythorne, S. C. Brown, J. C. Buettel, and B. W. Brook (2021). poems: R
475 package for simulating species’ range dynamics using pattern-oriented validation. *Methods*
476 *in Ecology and Evolution* 12(12), 2364–2371.

477 Forrest, D., M. Stuart, R. Batt, and M. Pinsky (2020, 06). pinskylab/oceanadapt: Update
478 2020.

479 Fredston, A., D. Ovando, L. da Cunha Godoy, J. Kong, B. Muffley, J. T. Thorson, and
480 M. Pinsky (2025). Dynamic range models improve the near-term forecast for a marine
481 species on the move. *Ecology Letters* 00, (under review).

482 Gabry, J., D. Simpson, A. Vehtari, M. Betancourt, and A. Gelman (2019). Visualization
483 in bayesian workflow. *Journal of the Royal Statistical Society: Series A (Statistics in*
484 *Society)* 182(2), 389–402.

485 Gabry, J., R. Češnovar, A. Johnson, and S. Bronder (2024). *cmdstanr: R Interface to Cmd-*
486 *Stan*. R package version 0.8.1.9000, commit f2e152b88fde5c2cde01ff078d5715b3b6248628.

487 Gaillard, J.-M. and J.-F. Lemaître (2020). An integrative view of senescence in nature.
488 *Functional Ecology* 34(1), 4–16.

489 Gneiting, T. and A. E. Raftery (2007). Strictly proper scoring rules, prediction, and estima-
490 tion. *Journal of the American statistical Association* 102(477), 359–378.

491 Healy, K., T. H. G. Ezard, O. R. Jones, R. Salguero-Gómez, and Y. M. Buckley (2019,
492 Aug). Animal life history is shaped by the pace of life and the distribution of age-specific
493 mortality and reproduction. *Nature Ecology & Evolution* 3(8), 1217–1224.

494 Heppell, S. S., H. Caswell, and L. B. Crowder (2000). Life histories and elasticity patterns:
495 perturbation analysis for species with minimal demographic data. *Ecology* 81(3), 654–665.

496 Hijmans, R. J., S. Phillips, J. Leathwick, and J. Elith (2024). *dismo: Species Distribution*
497 *Modeling*. R package version 1.3-16.

498 Hilborn, R. and C. J. Walters (2013). *Quantitative fisheries stock assessment: choice, dy-*
499 *namics and uncertainty*. Springer Science & Business Media.

500 Homan, M. D. and A. Gelman (2014, jan). The No-U-turn sampler: Adaptively setting
501 path lengths in hamiltonian Monte Carlo. *Journal of Machine Learning Research* 15(1),
502 1593–1623.

503 Johnson, K. F., C. Elizabeth, J. T. Thorson, E. Brooks, R. D. Methot, and A. E. Punt
504 (2016). Can autocorrelated recruitment be estimated using integrated assessment models
505 and how does it affect population forecasts? *Fisheries Research* 183, 222–232.

506 Karger, D. N., O. Conrad, J. Böhrner, T. Kawohl, H. Kreft, R. W. Soria-Auza, N. E. Zim-
507 mermann, H. P. Linder, and M. Kessler (2017, Sep). Climatologies at high resolution for
508 the earth’s land surface areas. *Scientific Data* 4(1), 170122.

509 Kearney, M. R., N. J. Briscoe, P. D. Mathewson, and W. P. Porter (2021). Nichemapr—an r
510 package for biophysical modelling: the endotherm model. *Ecography* 44(11), 1595–1605.

511 Kucukelbir, A., D. Tran, R. Ranganath, A. Gelman, and D. M. Blei (2017). Automatic
512 differentiation variational inference. *Journal of machine learning research* 18(14), 1–45.

513 Lambert, D. (1992). Zero-inflated Poisson regression, with an application to defects in
514 manufacturing. *Technometrics* 34(1), 1–14.

515 Landau, W. M. (2024). *instantiate: Pre-Compiled 'CmdStan' Models in R Packages*. R
516 package version 0.2.3.

517 Malchow, A.-K., G. Bocedi, S. C. F. Palmer, J. M. J. Travis, and D. Zurell (2021).
518 Rangeshiftr: an r package for individual-based simulation of spatial eco-evolutionary dy-
519 namics and species’ responses to environmental changes. *Ecography* 44(10), 1443–1452.

520 Malchow, A.-K., G. Fandos, U. G. Kormann, M. U. Gruebler, M. Kéry, F. Hartig, and
521 D. Zurell (2024). Fitting individual-based models of spatial population dynamics to long-
522 term monitoring data. *Ecological Applications* 34(4), e2966.

523 Markowska, K., K. Malinowska, and L. Kuczyński (2025). rangr: An R package for mech-
524 anistic, spatially explicit simulation of species range dynamics. *Methods in Ecology and*
525 *Evolution* 16(3), 468–476.

526 Maureaud, A. A., J. Palacios-Abrantes, Z. Kitchel, L. Mannocci, M. L. Pinsky, A. Fredston,
527 E. Beukhof, D. L. Forrest, R. Frelat, M. L. D. Palomares, L. Pecuchet, J. T. Thorson, P. D.
528 Van Denderen, and B. Mérigot (2024, January). FISHGLOB_data: an integrated dataset
529 of fish biodiversity sampled with scientific bottom-trawl surveys. *Scientific Data* 11(1),
530 24.

531 Monaghan, P., A. Charmantier, D. H. Nussey, and R. E. Ricklefs (2008, 03). The evolutionary
532 ecology of senescence. *Functional Ecology* 22(3), 371–378.

533 Morris, M., K. Wheeler-Martin, D. Simpson, S. J. Mooney, A. Gelman, and C. DiMaggio
534 (2019). Bayesian hierarchical spatial models: Implementing the Besag York Mollié model
535 in Stan. *Spatial and Spatio-temporal Epidemiology* 31, 100301.

536 Nenzén, H. K., R. M. Swab, D. A. Keith, and M. B. Araújo (2012). demoniche—an R-package
537 for simulating spatially-explicit population dynamics. *Ecography* 35(7), 577–580.

538 Pagel, J. and F. M. Schurr (2012). Forecasting species ranges by statistical estimation of
539 ecological niches and spatial population dynamics. *Global Ecology and Biogeography* 21(2),
540 293–304.

541 Paradinas, I., J. Illian, and S. Smout (2023, 05). Understanding spatial effects in species
542 distribution models. *PLOS ONE* 18(5), 1–6.

543 Pebesma, E. (2018). Simple features for R: standardized support for spatial vector data.
544 *The R Journal* 10(1), 439–446.

545 Pecl, G. T., M. B. Araújo, J. D. Bell, J. Blanchard, T. C. Bonebrake, I.-C. Chen, T. D. Clark,
546 R. K. Colwell, F. Danielsen, B. Evengård, L. Falconi, S. Ferrier, S. Frusher, R. A. Garcia,
547 R. B. Griffis, A. J. Hobday, C. Janion-Scheepers, M. A. Jarzyna, S. Jennings, J. Lenoir,
548 H. I. Linnetved, V. Y. Martin, P. C. McCormack, J. McDonald, N. J. Mitchell, T. Mu-
549 stonen, J. M. Pandolfi, N. Pettorelli, E. Popova, S. A. Robinson, B. R. Scheffers, J. D.
550 Shaw, C. J. B. Sorte, J. M. Strugnell, J. M. Sunday, M.-N. Tuanmu, A. Vergés, C. Vil-
551 lanueva, T. Wernberg, E. Wapstra, and S. E. Williams (2017). Biodiversity redistribution
552 under climate change: Impacts on ecosystems and human well-being. *Science* 355(6332),
553 eaai9214.

554 Pinsky, M. L., G. Reygondeau, R. Caddell, J. Palacios-Abrantes, J. Spijkers, and W. W. L.
555 Cheung (2018). Preparing ocean governance for species on the move. *Science* 360(6394),
556 1189–1191.

557 R Core Team (2024). *R: A Language and Environment for Statistical Computing*. Vienna,
558 Austria: R Foundation for Statistical Computing. version: 4.4.1.

559 Sauer, J. R., J. E. Fallon, and R. Johnson (2003). Use of north american breeding bird
560 survey data to estimate population change for bird conservation regions. *The Journal of*
561 *Wildlife Management* 67(2), 372–389.

562 Serra-Diaz, J. M., J. Franklin, W. W. Dillon, A. D. Syphard, F. W. Davis, and R. K.
563 Meentemeyer (2016). California forests show early indications of both range shifts and
564 local persistence under climate change. *Global Ecology and Biogeography* 25(2), 164–175.

565 Shackelford, C. E., R. E. Brown, and R. N. Conner (2000, January). Red-bellied woodpecker
566 (*melanerpes carolinus*). *The Birds of North America Online*.

567 Sullivan, B. L., C. L. Wood, M. J. Iliff, R. E. Bonney, D. Fink, and S. Kelling (2009).
568 eBird: A citizen-based bird observation network in the biological sciences. *Biological*
569 *Conservation* 142(10), 2282–2292.

570 Thorson, J. T., S. C. Anderson, P. Goddard, and C. N. Rooper (2025). tinyVAST: R package
571 with an expressive interface to specify lagged and simultaneous effects in multivariate
572 spatio-temporal models. *Global Ecology and Biogeography* 34(4), e70035.

573 Thorson, J. T., S. J. Barbeaux, D. R. Goethel, K. A. Kearney, E. A. Laman, J. K. Nielsen,
574 M. R. Siskey, K. Siwicke, and G. G. Thompson (2021). Estimating fine-scale movement
575 rates and habitat preferences using multiple data sources. *Fish and Fisheries* 22(6), 1359–
576 1376.

577 Urban, M. C., G. Bocedi, A. P. Hendry, J.-B. Mihoub, G. Pe'er, A. Singer, J. R. Bridle, L. G.
578 Crozier, L. D. Meester, W. Godsoe, A. Gonzalez, J. J. Hellmann, R. D. Holt, A. Huth,
579 K. Johst, C. B. Krug, P. W. Leadley, S. C. F. Palmer, J. H. Pantel, A. Schmitz, P. A.
580 Zollner, and J. M. J. Travis (2016). Improving the forecast for biodiversity under climate
581 change. *Science* 353(6304), aad8466.

582 Uribe-Rivera, D. E., G. Guillera-Arroita, S. M. Windecker, P. Plissock, and B. A. Wintle
583 (2023). The predictive performance of process-explicit range change models remains largely
584 untested. *Ecography* 2023(4), e06048.

585 Vehtari, A., A. Gelman, and J. Gabry (2017). Practical Bayesian model evaluation using
586 leave-one-out cross-validation and WAIC. *Statistics and computing* 27, 1413–1432.

587 Vehtari, A., A. Gelman, D. Simpson, B. Carpenter, and P.-C. Bürkner (2021). Rank-
588 normalization, folding, and localization: An improved \hat{R} for assessing convergence of
589 MCMC (with discussion). *Bayesian Analysis* 16(2), 667–718.

590 Ye, T., V. H. Lachos, X. Wang, and D. K. Dey (2021). Comparisons of zero-augmented

591 continuous regression models from a Bayesian perspective. *Statistics in Medicine* 40(5),
592 1073–1100.

593 Yee, T. W. (2014). Reduced-rank vector generalized linear models with two linear predictors.
594 *Computational Statistics & Data Analysis* 71, 889–902.

595 Zhang, L., B. Carpenter, A. Gelman, and A. Vehtari (2022). Pathfinder: Parallel quasi-
596 newton variational inference. *Journal of Machine Learning Research* 23(306), 1–49.

597 Ziolkowski Jr, D., M. Lutmerding, V. Aponte, and M. Hudson (2024). North American
598 breeding bird survey dataset 1966–2023. *US Geological Survey data release*. [https://doi.](https://doi.org/10.5066/P97WAZE5)
599 [org/10.5066/P97WAZE5](https://doi.org/10.5066/P97WAZE5).